A Tube-based MPC Scheme for Interaction Control of Underwater Vehicle Manipulator Systems

Alexandros Nikou, Christos K. Verginis and Dimos V. Dimarogonas
Department of Automatic Control
School of Electrical Engineering and Computer Science
KTH Royal Institute of Technology, Stockholm, Sweden
{anikou,cverginis,dimos}@kth.se

***Abstract*—Over the last years, the development of Autonomous Underwater Vehicles (AUV) with attached robotic manipulators, the so-called Underwater Vehicle Manipulator System (UVMS), has gained significant research attention, due to the ability of interaction with underwater environments. In such applications, force/torque controllers which guarantee that the end-effector of the UVMS applies desired forces/torques towards the environment, should be designed in a way that state and input constraints are taken into consideration. Furthermore, due to their complicated structure, unmodeled dynamics as well as external disturbances may arise. Motivated by this, we proposed a robust Model Predicted Control Methodology (NMPC) methodology which can handle the aforementioned constraints in an efficient way and it guarantees that the end-effector is exerting the desired forces/torques towards the environment. Simulation results verify the validity of the proposed framework.**

I. Introduction

Most of the underwater manipulation tasks, such as maintenance of ships, underwater weld inspection, surveying oil/gas searching, require the manipulator mounted on the vehicle to be in contact with the underwater object or environment (see [1]–[6]). The aforementioned tasks are usually complex due to highly nonlinear dynamics, the presence of uncertainties, external disturbances as well as state and control input (actuation) constraints. Thus, these constraints should be taken into account in the force control design process in an efficient way.

Motivated by the aforementioned, this paper considers the modeling of a general UVMS in compliant contact with a planar surface, and the development of a constrained Nonlinear Model Predictive Control (NMPC) scheme for force/torque control. NMPC for manipulation of nominal system dynamics has been proposed in [5], [7] for stabilization of ground vehicles with attached manipulators to pre-defined positions. In this work, we propose a novel robust tube-based NMPC force control approach that efficiently deals with state and input constraints and achieves a desired exerted force from the UVMS to the environment. In particular, the controller consists of two terms: a nominal control input, which is computed on-line and is the outcome of a Finite Horizon Optimal Control Problem (FHOCP) that is repeatedly solved at every sampling time, for its nominal system dynamics; and an additive state feedback law which is computed off-line and guarantees that the real trajectory of the closed-loop system will belong to a hyper-tube centered along the nominal trajectory. The volume of the hyper-tube depends on the upper bound of the disturbances, the bounds of the Jacobian matrix as well as Lipschitz constants of the UVMS dynamics. Under the assumption that the FHOCP is feasible at time $t = 0$, we guarantee the boundedness of the closed-loop system states.

The rest of this manuscript is structured as follows: Section II provides the notation that will be used as well as necessary background knowledge; in Section III, the problem treated in this paper is formally defined; Section IV contains the main results of the paper; Section V is devoted to numerical simulations; and in Section VI, conclusions and future research directions are discussed.

This work was supported by the H2020 ERC Grant BUCOPHSYS, the EU H2020 Co4Robots project, the Swedish Foundation for Strategic Research (SSF), the Swedish Research Council (VR) and the Knut och Alice Wallenberg Foundation (KAW).

II. Notation and Preliminaries

Define by $\mathbb{N}$ and $\mathbb{R}$ the sets of positive integers and real numbers, respectively. Given the set $\mathcal{S}$, define by $S^n \coloneqq S \times \cdots \times S$, its n-fold Cartesian product. Given vector $z \in \mathbb{R}^n$ define by

$$\|z\|_2 \coloneqq \sqrt{z^\top z}, \quad \|z\|_P \coloneqq \sqrt{z^\top P z},$$

its Euclidean and weighted norm, with $P \geq 0$. Given vectors $z_1,\ z_2 \in \mathbb{R}^3$, $\mathcal{S} : \mathbb{R}^3 \to \mathfrak{so}(3)$ stands for the skew-symmetric matrix defined according to $\mathcal{S}(z_1)z_2 = z_1 \times z_2$ where

$$\mathfrak{so}(3) \coloneqq \left\{\mathcal{S} \in \mathbb{R}^{3\times 3} : z^\top \mathcal{S}(\cdot) z = 0, \forall z \in \mathbb{R}^3\right\}.$$

$\lambda_{\min}(P)$ stands for the minimum absolute value of the real part of the eigenvalues of $P \in \mathbb{R}^{n\times n}$; $0_{m\times n} \in \mathbb{R}^{m\times n}$ and $I_n \in \mathbb{R}^{n\times n}$ stand for the $m \times n$ matrix with all entries zeros and the identity matrix, respectively. Given coordination frames Σ_i, Σ_j, denote by R_i^j the transformation from Σ_i to Σ_j. Given sets $\mathcal{S}_1$, $\mathcal{S}_2 \subseteq \mathbb{R}^n$, $\mathcal{S} \subseteq \mathbb{R}^m$ and matrix $B \in \mathbb{R}^{n\times m}$, the *Minkowski addition*, the *Pontryagin difference* and the *matrix-set multiplication* are respectively defined by:

$$\begin{aligned}\mathcal{S}_1 \oplus \mathcal{S}_2 &\coloneqq \{s_1 + s_2 : s_1 \in \mathcal{S}_1, s_2 \in \mathcal{S}_2\},\\ \mathcal{S}_1 \ominus \mathcal{S}_2 &\coloneqq \{s_1 : s_1 + s_2 \in \mathcal{S}_1, \forall s_2 \in \mathcal{S}_2\},\\ B \circ \mathcal{S} &\coloneqq \{b : b = Bs, s \in \mathcal{S}\}.\end{aligned}$$

Lemma 1. *[8] For any constant $\rho > 0$, vectors $z_1,\ z_2 \in \mathbb{R}^n$ and matrix $P \in \mathbb{R}^{n\times n}$, $P > 0$ it holds that*

$$z_1 P z_2 \leq \tfrac{1}{4\rho} z_1^\top P z_1 + \rho z_2^\top P z_2.$$

Definition 1. [8] Consider a dynamical system $\dot{\chi} = f(\chi, u, d)$ where: $\chi \in \mathcal{X}$, $u \in \mathcal{U}$, $d \in \mathcal{D}$ with initial condition $\chi(0) \in \mathcal{X}$. A set $\mathcal{X}' \subseteq \mathcal{X}$ is a *Robust Control Invariant (RCI) set* for the system, if there exists a feedback control law $u := \kappa(\chi) \in \mathcal{U}$, such that for all $\chi(0) \in \mathcal{X}'$ and for all $d \in \mathcal{D}$ it holds that $\chi(t) \in \mathcal{X}'$ for all $t \geq 0$, along every solution $\chi(t)$.

III. Problem Formulation

A. Kinematic Model

Consider a UVMS which is composed of an AUV and a n Degree Of Freedom (DoF) manipulator mounted on the base of the vehicle. The AUV can be considered as a six DoF rigid body with position and orientation vector $\eta := [x, y, z \mid \phi, \theta, \psi]^\top \in \mathbb{R}^6$, where the components of the vectors have been named according to SNAME [9] as surge, sway, heave, roll, pitch and yaw respectively. The joint angular position state vector of the manipulator is defined by $q := [q_1, \ldots, q_n]^\top \in \mathbb{R}^n$. Define by $\dot{q} := [\dot{q}_1, \ldots, \dot{q}_n]^\top \in \mathbb{R}^n$ the corresponding joint velocities.

In order to describe the motion of the combined system, the earth-fixed inertial frame Σ_I, the body-fixed frame Σ_B and the end-effector fixed frame Σ_E are introduced (see Fig. 1). Moreover, without loss of generality, the reference frame Σ_0 is chosen to be located at the manipulator's base, and the frames $\Sigma_1, \ldots, \Sigma_n$ are located to the 1-st, $\ldots$, n-th link of the manipulator, respectively, under the Denavit-Hartenberg convention [10]. The translational and rotational kinematic equations for the AUV system (see [1], [11]) are given by:

$$\dot{\eta} = \begin{bmatrix} \dot{\eta}_1 \\ \dot{\eta}_2 \end{bmatrix} = \mathfrak{J}(\eta_2) \begin{bmatrix} \nu_1 \\ \nu_2 \end{bmatrix}, \tag{1a}$$

$$\mathfrak{J}(\eta_2) := \begin{bmatrix} \mathfrak{J}_1(\eta_2) & 0_{3\times3} \\ 0_{3\times3} & \mathfrak{J}_2(\eta_2) \end{bmatrix}, \tag{1b}$$

$$\mathfrak{J}_1(\eta_2) := \begin{bmatrix} c_\theta c_\psi & s_\phi s_\theta c_\psi - s_\psi c_\phi & s_\theta c_\phi c_\psi + s_\phi s_\psi \\ s_\psi c_\theta & s_\phi s_\theta s_\psi + c_\phi c_\psi & s_\theta s_\psi c_\phi - s_\phi c_\psi \\ -s_\theta & s_\phi c_\theta & c_\phi c_\theta \end{bmatrix}, \tag{1c}$$

$$\mathfrak{J}_2(\eta_2) := \begin{bmatrix} 1 & \frac{s_\phi s_\theta}{c_\theta} & \frac{c_\phi s_\theta}{c_\theta} \\ 0 & c_\phi & -s_\phi \\ 0 & \frac{s_\phi}{c_\theta} & \frac{c_\phi}{c_\theta} \end{bmatrix}, \tag{1d}$$

where $\eta_1 := [x, y, z]^\tau \in \mathbb{R}^3$, $\eta_2 := [\phi, \theta, \psi]^\top \in \mathbb{R}^3$ denote the position vector and the orientation vector of the frame Σ_B relative to the frame Σ_I, respectively; $\nu_1, \nu_2 \in \mathbb{R}^3$ denote the linear and the angular velocity of the frame Σ_B with respect to Σ_I respectively; $\mathfrak{J}(\eta_2) \in \mathbb{R}^{6\times6}$ stands for the Jacobian matrix transforming the velocities from Σ_B to Σ_I; $\mathfrak{J}_1(\eta_2)$, $\mathfrak{J}_2(\eta_2) \in \mathbb{R}^{3\times3}$ are the corresponding parts of the Jacobian related to position and orientation, respectively; The notation s_ς and c_ς stand for the trigonometric functions $\sin(\varsigma)$ and $\cos(\varsigma)$ of an angle $\varsigma \in \mathbb{R}$, respectively.

Denote by

$$\mathfrak{q} := \left[\eta_1^\top, \eta_2^\top, q^\top\right]^\top \in \mathbb{R}^{6+n},$$

the pose configuration vector of the UVMS. Let $\mathfrak{p}$, $\mathfrak{o} \in \mathbb{R}^3$ be the position and orientation vectors of the end-effector

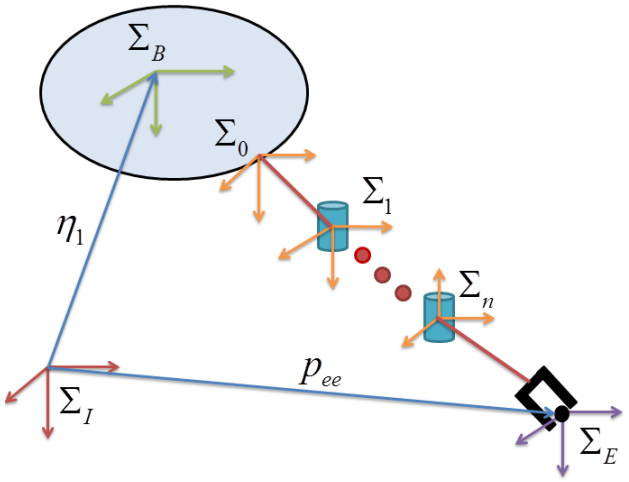

Fig. 1: An AUV Equipped with a n DoF manipulator

with reference to the frame Σ_I, respectively. The vectors $\mathfrak{p}$, $\mathfrak{o}$ depend on the pose $\mathfrak{q}$ and they can be obtained by the the following homogeneous transformation:

$$\mathfrak{T}(\mathfrak{q}) := \begin{bmatrix} R_E^I(\mathfrak{q}) & \mathfrak{p}(\mathfrak{q}) \\ 0_{1\times3} & 1 \end{bmatrix} = T_B^I T_0^B T_1^0 \cdots T_n^{n-1} T_E^n, \tag{2}$$

where: T_i^j is the homogeneous transformation matrix describing the position and orientation of frame Σ_i with reference to the frame Σ_j with $i, j \in \{1, \ldots, n, I, 0, B, E\}$. The end-effector linear velocity $\dot{\mathfrak{p}} \in \mathbb{R}^3$ and the time derivative or Euler angles $\dot{\mathfrak{o}} \in \mathbb{R}^3$ are related to the body-fixed velocities ν_1, ν_2 and $\dot{q}$ with the following *kinematics model:*

$$\dot{\chi} = J(\mathfrak{q})\zeta, \tag{3}$$

where

$$\chi := [\mathfrak{p}^\top, \mathfrak{o}^\top]^\top \in \mathbb{R}^6, \quad \zeta := \left[\nu_1^\top, \nu_2^\top, \dot{q}^\top\right]^\top \in \mathbb{R}^{6+n},$$

is the body-fixed system velocity vector. The Jacobian transformations matrices

$$J(\mathfrak{q}) \in \mathbb{R}^{6\times(6+n)}, \quad J_{\text{pos}}(\mathfrak{q}) \in \mathbb{R}^{3\times(6+n)}, \quad J_{\text{or}}(\mathfrak{q}) \in \mathbb{R}^{3\times(6+n)},$$

are respectively defined by:

$$J(\mathfrak{q}) := \begin{bmatrix} J_{\text{pos}}(\mathfrak{q}) \\ J_{\text{or}}(\mathfrak{q}) \end{bmatrix},$$
$$J_{\text{pos}}(\mathfrak{q}) := \left[\mathfrak{J}_1(\eta_2) \,\middle|\, -\mathfrak{J}_1(\eta_2)\mathcal{S}(p_{ee}) \,\middle|\, R_0^I J_{e,1}\right],$$
$$J_{\text{or}}(\mathfrak{q}) := \left[0_{3\times3} \,\middle|\, \mathfrak{J}_2(\mathfrak{o})R_B^E \,\middle|\, \mathfrak{J}_2(\mathfrak{o})R_0^E J_{e,2}\right].$$

In the latter, the vector $p_{ee} \in \mathbb{R}^3$ is the local position of the end-effector with reference to the frame Σ_B; the matrices $J_{e,1}$, $J_{e,2} \in \mathbb{R}^{3\times n}$ represent the manipulator Jacobian matrices with respect to the frame Σ_0; and $\mathcal{S}(\cdot)$ the skew-symmetric matrix as given in Section II. For the aforementioned transformations we refer to [10].

B. Dynamic Model

When the end-effector of the robotic system is in contact with the environment, the force at the tip of the manipulator acts on the whole system according to the following uncertain nonlinear dynamics:

$$\dot{\zeta} = f(\chi, \zeta) + \mathfrak{u} + d(\mathfrak{q}, \zeta, t), \tag{4}$$

where:

$$f(\chi, \zeta) \coloneqq \\ -M(\mathfrak{q})^{-1}\Big\{C(\zeta, \mathfrak{q})\zeta + D(\zeta, \mathfrak{q})\zeta + g(\mathfrak{q}) + J^{\top}(\mathfrak{q})\mathfrak{F}(\chi)\Big\}, \tag{5}$$

where $M(\mathfrak{q}) \in \mathbb{R}^{(6+n)\times(6+n)}$ is the inertia matrix for which it holds that: $z^{\top}M(\mathfrak{q})z > 0$, $\forall z \in \mathbb{R}^{6+n}$; $C(\zeta, \mathfrak{q}) \in \mathbb{R}^{(6+n)\times(6+n)}$ is the matrix of Coriolis and centripetal terms; $D(\zeta, \mathfrak{q}) \in \mathbb{R}^{(6+n)\times(6+n)}$ is the matrix of dissipative effects; $d(\mathfrak{q}, \zeta, t) \in \mathbb{R}^{6+n}$ is a vector that models the external disturbances, uncertainties and unmodeled dynamics of the system; $g(\mathfrak{q}) \in \mathbb{R}^{(6+n)}$ is the vector of gravity and buoyancy effects; $\mathfrak{u} \in \mathbb{R}^{6+n}$ denotes the vector of the propulsion forces and moments acting on the vehicle in the frame Σ_B as well as the joint torques; $\mathfrak{F}(\chi) \in \mathbb{R}^6$ is the vector of interaction forces and torques exerted by the end-effector towards the environment expressed in Σ_I.

In this paper, an interaction between the end-effector and a frictionless, elastically compliant surface is assumed. Then, according to [12], the vector of interaction forces and torques that is exerted by the end-effector can be written as:

$$\mathfrak{F}(\chi) \coloneqq K(\chi - \chi_{\text{eq}}), \tag{6}$$

where $K \in \mathbb{R}^{6\times6}$, $K > 0$ stands for the stiffness matrix, which represents elastic coefficient of the environment, and $\chi_{\text{eq}} \in \mathbb{R}^6$ is the given constant vector of the equilibrium position/orientation of the undeformed environment.

We also consider that the UVMS is in the presence of state and input constraints given by $\mathfrak{q} \in \mathcal{Q}$, $\zeta \in \mathcal{Z}$, $u \in \mathcal{U}$, where $\mathcal{Q} \subseteq \mathbb{R}^{6+n}$, $\mathcal{Z} \subseteq \mathbb{R}^{6+n}$ and $\mathcal{U} \subseteq \mathbb{R}^{6+n}$ are *connected sets containing the origin*. For certain technical reasons that will be presented thereafter, the constraints imposed to the configuration states $\mathfrak{q}$ are given by:

$$\mathcal{Q} \coloneqq \Big\{\mathfrak{q} \in \mathbb{R}^{6+n} : \lambda_{\min}\left[\tfrac{J^{+}(\mathfrak{q})+J^{+}(\mathfrak{q})^{\top}}{2}\right] \geq \underline{J}, \\ \|J(\mathfrak{q})\|_2 \leq \overline{J},\ \|\dot{J}(\mathfrak{q})\|_2 \leq \widetilde{J}\Big\}, \tag{7}$$

where $J^{+}(\mathfrak{q}) \coloneqq J(\mathfrak{q})J(\mathfrak{q})^{\top}$ and $\underline{J}$, $\overline{J}$, $\widetilde{J} > 0$. According to (2), the constraints $\mathfrak{q} \in \mathcal{Q}$ impose also constraints on the vector $\chi \in \mathcal{X} \subseteq \mathbb{R}^6$, where the set $\mathcal{X}$ can be computed by the transformation $\mathfrak{T}(\mathfrak{q})$, as given in (2). Note also that the function f given in (5) is continuously differentiable in the set $\mathcal{Q} \times \mathcal{X} \times \mathcal{Z}$. Furthermore, assume bounded disturbances $d \in \mathcal{D}$ where: $\mathcal{D} \coloneqq \big\{d \in \mathbb{R}^{6+n} : \|d(\mathfrak{q}, \zeta, t)\|_2 \leq \widetilde{d},\ \forall(\mathfrak{q}, \zeta) \in \mathcal{Q} \times \mathcal{Z}\big\}$, where $\widetilde{d} > 0$.

For the kinematics/dynamics (3),(4), define the corresponding *nominal kinematics/dynamics* by:

$$\dot{\overline{\chi}} = J(\overline{\mathfrak{q}})\overline{\zeta}, \tag{8a}$$

$$\dot{\overline{\zeta}} = f(\overline{\chi}, \overline{\zeta}) + \overline{u}, \tag{8b}$$

where $d(\cdot) \equiv 0$, $\overline{\mathfrak{q}} \in \mathcal{Q}$, $\overline{\chi} \in \mathcal{X}$, $\overline{\zeta} \in \mathcal{Z}$ and $\overline{u} \in \mathcal{U}$. Define the stack vector $\overline{\xi} \coloneqq [\overline{\chi}, \overline{\zeta}]^{\top} \in \mathbb{R}^{12+n}$ and consider the linear nominal system $\dot{\overline{\xi}} = A\overline{\xi} + B\overline{u}$, $A \in \mathbb{R}^{(12+n)\times(12+n)}$, $B \in \mathbb{R}^{(12+n)\times(6+n)}$, which is the outcome of the Jacobian linearization of the nominal dynamics (8a),(8b) around the equilibrium point $\xi = 0$. Due to the dimension of the control input ($6 + n > 6$), the stabilization of the state $\overline{\chi}$ to the desired state χ_{des} can be achieved. Therefore, the linear system is stabilizable.

C. Problem Statement

Problem 1. Consider a UVMS composed of an AUV and an attached manipulator with n DoF, which is in contact with a surface of a compliant environment. The UVMS is governed by the kinematics and dynamics models given in (3) and (4), respectively. The system is in the presence of state and input constraints as well as bounded disturbances which are respectively given by:

$$\mathfrak{q} \in \mathcal{Q},\ \chi \in \mathcal{X},\ \zeta \in \mathcal{Z},\ \mathfrak{u} \in \mathcal{U},\ d \in \mathcal{D}. \tag{9}$$

Given a vector $\mathfrak{F}_{\text{des}} \in \mathbb{R}^6$ that satisfies (6) and stands for the desired force/torque vector that the end-effector is required to exert towards a surface of the environment, design a *feedback control law* $\mathfrak{u} \coloneqq \kappa(\chi, \zeta)$ such that $\lim_{t\to\infty} \|\mathfrak{F}(\chi(t)) - \mathfrak{F}_{\text{des}}\|_2 \to 0$, while all the constraints given in (9) are satisfied.

IV. Main Results

In this section, we propose a novel feedback control law that solves Problem 1 in a systematic way. Due to the fact that it is required to design a feedback control law that guarantees the minimization of the term $\|\mathfrak{F}(t) - \mathfrak{F}_{\text{des}}\|_2$, as $t \to \infty$, under state and input constraints given by (9), we utilize a Nonlinear Model Predictive Control (NMPC) framework [13]–[18]. Furthermore, since the UVMS is under the presence of disturbances/uncertainties $d \in \mathcal{D}$, we provide a robust analysis, the so-called tube-based robust NMPC approach [8], [19], [20]. In particular, first, the error states and the corresponding transformed constraints sets are defined in Section IV-A. Then, the proposed feedback control law consists of two parts: an on-line control law which is the outcome of a solution to a Finite Horizon Optimal Control Problem (FHOCP) for the nominal system dynamics (see Section IV-C); and a state feedback law which is designed off-line and guarantees that the real system trajectories always lie within a hyper-tube centered along the nominal trajectories (see IV-B).

A. Errors and Constraints

According to (6), for the error between the actual $\mathfrak{F}$ and the desired $\mathfrak{F}_{\text{des}}$ forces/torques exerted from the end-effector to the surface it holds that: $\mathfrak{F} - \mathfrak{F}_{\text{des}} = K(\chi - \chi_{\text{eq}}) - K(\chi_{\text{des}}$

$-\chi_{\text{eq}}) = K(\chi - \chi_{\text{des}})$, where $\chi_{\text{des}} \coloneqq K^{-1}\mathfrak{F}_{\text{des}} + \chi_{\text{eq}} \in \mathbb{R}^6$. The latter implies that if we design a feedback control law $u = \kappa(\chi, \zeta)$ which guarantees that $\lim_{t\to\infty} \|\chi(t) - \chi_{\text{des}}\|_2 \to 0$, while all the constraints given in (9) are satisfied, Problem 1 will have been solved.

Define the error state $e \coloneqq \chi - \chi_{\text{des}} \in \mathbb{R}^6$. Then, the *uncertain error kinematics/dynamics* are given by:

$$\dot{e} = J(\mathfrak{q})\zeta, \tag{10a}$$

$$\dot{\zeta} = f(e + \chi_{\text{des}}, \zeta) + \mathfrak{u} + d(\mathfrak{q}, \zeta, t), \tag{10b}$$

and the corresponding *nominal error kinematics/dynamics* by:

$$\dot{\overline{e}} = J(\overline{\mathfrak{q}})\overline{\zeta}, \tag{11a}$$

$$\dot{\overline{\zeta}} = f(\overline{e} + \chi_{\text{des}}, \overline{\zeta}) + \overline{u}, \tag{11b}$$

In order to translate the constraints for the state $\chi \in \mathcal{X}$ to constraints that are dictated regarding the error e, the constraints set $\mathcal{E} \coloneqq \{e \in \mathbb{R}^6 : e \in \mathcal{X} \oplus (-\chi_{\text{des}})\}$ is introduced.

B. Feedback Control Design

Consider the feedback law:

$$\mathfrak{u} \coloneqq \overline{u}(\overline{e}, \overline{\zeta}) + \kappa(e, \zeta, \overline{e}, \overline{\zeta}), \tag{12}$$

which consists of a nominal control law $\overline{u}(\overline{e}, \overline{\zeta}) \in \mathcal{U}$ and a state feedback law $\kappa(\cdot)$. The control action $\overline{u}(\overline{e}, \overline{\zeta})$ will be the outcome of a FHOCP for the nominal kinematics/dynamics (11a),(11b) which is solved on-line at each sampling time. The state feedback law $\kappa(\cdot)$ is used to guarantee that the real trajectories $e(t)$, $\zeta(t)$, which are the solution to (10a),(10b), always remain within a bounded hyper-tube centered along the nominal trajectories $\overline{e}(t)$, $\overline{\zeta}(t)$ which are the solution to (11a),(11b).

Define by $\mathfrak{e} \coloneqq e - \overline{e} \in \mathbb{R}^6$ and $\mathfrak{z} \coloneqq \zeta - \overline{\zeta} \in \mathbb{R}^{6+n}$ the deviation between the real states of the uncertain system (10a),(10b) and the states of the nominal system (11a),(11b), respectively, with $\mathfrak{e}(0) = \mathfrak{z}(0) = 0$. It will be proved hereafter that the trajectories $\mathfrak{e}(t)$, $\mathfrak{z}(t)$ remain invariant in compact sets. The dynamics of the states $\mathfrak{e}$, $\mathfrak{z}$ are written as:

$$\dot{\mathfrak{e}} = \mathfrak{b}(\chi, \overline{\chi}, \zeta) + J(\overline{\mathfrak{q}})\mathfrak{z}, \tag{13a}$$

$$\dot{\mathfrak{z}} = \mathfrak{l}(e, \overline{e}, \zeta, \overline{\zeta}) + (\mathfrak{u} - \overline{u}) + d(\mathfrak{q}, \zeta, t), \tag{13b}$$

where the functions $\mathfrak{b}$, $\mathfrak{l}$ are defined by: $\mathfrak{b}(\chi, \overline{\chi}, \zeta) \coloneqq \mathfrak{c}(\chi, \zeta) - \mathfrak{c}(\overline{\chi}, \zeta)$, $\mathfrak{l}(e, \overline{e}, \zeta, \overline{\zeta}) \coloneqq f(e + \chi_{\text{des}}, \zeta) - f(\overline{e} + \chi_{\text{des}}, \overline{\zeta})$, with $\mathfrak{c}(\chi, \zeta) \coloneqq J(\mathfrak{q})\zeta$. Since the aforementioned functions are continuously differentiable, the following hold:

$$\begin{aligned}
\|\mathfrak{b}(\cdot)\|_2 &= \|\mathfrak{c}(\chi, \zeta) - \mathfrak{c}(\overline{\chi}, \zeta)\|_2 \leq L_{\mathfrak{c}}\|\chi - \overline{\chi}\|_2 = L_{\mathfrak{c}}\|\mathfrak{e}\|_2, \\
\|\mathfrak{l}(\cdot)\|_2 &\leq \|f(e + \chi_{\text{des}}, \zeta) - f(\overline{e} + \chi_{\text{des}}, \zeta)\|_2 \\
&\quad + \|f(\overline{e} + \chi_{\text{des}}, \zeta) - f(\overline{e} + \chi_{\text{des}}, \overline{\zeta})\|_2 \\
&\leq L_1\|e - \overline{e}\|_2 + L_2\|\zeta - \overline{\zeta}\|_2 \leq L\left(\|\mathfrak{e}\|_2 + \|\mathfrak{z}\|_2\right).
\end{aligned}$$

The constant $L_{\mathfrak{c}}$ stands for the Lipschitz constant of function $\mathfrak{c}$ with respect to the variable χ; L_1, L_2 stand for the Lipschitz constants of function h with respect to the variables χ and ζ, respectively, and $L \coloneqq \max\{L_1, L_2\}$.

Lemma 2. *The state feedback law designed by:*

$$\kappa(e, \overline{e}, \zeta, \overline{\zeta}) \coloneqq -k(e - \overline{e}) - k\sigma J(\overline{\mathfrak{q}})^\top(\zeta - \overline{\zeta}), \tag{14}$$

where k, $\sigma > 0$ are chosen such that the following hold:

$$\underline{\sigma} > 0, \quad \sigma \coloneqq \frac{L_{\mathfrak{c}} + \underline{\sigma}}{\underline{J}}, \quad \rho > \tfrac{\Lambda_1}{4\underline{\sigma}}, \quad k > \rho\Lambda_1 + \Lambda_2, \tag{15a}$$

$$\Lambda_1 \coloneqq \left[L + \overline{J} + \sigma\left(L_{\mathfrak{c}} + \widetilde{J}\right)\right], \Lambda_2 \coloneqq \left(L + \sigma\overline{J}^2\right), \tag{15b}$$

renders the sets:

$$\Omega_1 \coloneqq \left\{\mathfrak{e} \in \mathbb{R}^6 : \|\mathfrak{e}\|_2 \leq \tfrac{\widetilde{d}}{\min\{\alpha_1, \alpha_2\}}\right\}, \tag{16a}$$

$$\Omega_2 \coloneqq \left\{\mathfrak{z} \in \mathbb{R}^{6+n} : \|\mathfrak{z}\|_2 \leq \tfrac{2\widetilde{d}}{\overline{J}\min\{\alpha_1, \alpha_2\}}\right\}, \tag{16b}$$

RCI sets for the error dynamics (13a)*,* (13b)*, according to Definition 1. The constants α_1, $\alpha_2 > 0$ are defined by:*

$$\alpha_1 \coloneqq \underline{\sigma} - \tfrac{\Lambda_1}{4\rho}, \ \alpha_2 \coloneqq k - \rho\Lambda_1 - \Lambda_2. \tag{17}$$

Proof : A backstepping control methodology will be used [21]. The state $\mathfrak{z}$ in (13a) can be seen as virtual input to be designed such that the Lyapunov function $\mathfrak{L}_1(\mathfrak{e}) \coloneqq \frac{1}{2}\|\mathfrak{e}\|_2^2$ for the system (13a) is always decreasing. The time derivative of $\mathfrak{L}_1$ along the trajectories of system (13a) is given by:

$$\dot{\mathfrak{L}}(\mathfrak{e}) = \mathfrak{e}^\top J(\overline{\mathfrak{q}})\mathfrak{z} + \mathfrak{e}^\top\mathfrak{b}(\cdot) \leq \mathfrak{e}^\top J(\overline{\mathfrak{q}})\mathfrak{z} + L_{\mathfrak{c}}\|\mathfrak{e}\|_2^2. \tag{18}$$

Design the virtual control input as $\mathfrak{z} \equiv -\sigma J(\overline{\mathfrak{q}})^\top\mathfrak{e}$, with $\underline{J}$, σ as given in (7), (15a), respectively. Then, by employing (7), (18) becomes:

$$\begin{aligned}
\dot{\mathfrak{L}}(\mathfrak{e}) &\leq -\sigma\mathfrak{e}^\top J^+(\overline{\mathfrak{q}})\mathfrak{e} + L_{\mathfrak{c}}\|\mathfrak{e}\|_2^2 \\
&\leq -\sigma\lambda_{\min}\left[\tfrac{J^+(\overline{\mathfrak{q}}) + J^+(\overline{\mathfrak{q}})^\top}{2}\right]\|\mathfrak{e}\|_2^2 + L_{\mathfrak{c}}\|\mathfrak{e}\|_2^2 \\
&\leq -\sigma\underline{J}\|\mathfrak{e}\|_2^2 + L_{\mathfrak{c}}\|\mathfrak{e}\|_2^2 = -\underline{\sigma}\|\mathfrak{e}\|_2^2.
\end{aligned} \tag{19}$$

Define the backstepping auxiliary error state $\mathfrak{r} \coloneqq \mathfrak{z} + \sigma J(\overline{\mathfrak{q}})^\top\mathfrak{e} \in \mathbb{R}^{6+n}$ and the the stack vector $\mathfrak{y} \coloneqq [\mathfrak{e}^\top, \mathfrak{r}^\top]^\top \in \mathbb{R}^{12+n}$. Consider the Lyapunov function $\mathfrak{L}(\mathfrak{y}) = \frac{1}{2}\|\mathfrak{y}\|^2$. Its time derivative along the trajectories of the system (13a),(13b) is given by:

$$\begin{aligned}
\dot{\mathfrak{L}}(\mathfrak{y}) &= \mathfrak{e}^\top\dot{\mathfrak{e}} + \mathfrak{r}^\top\left[\dot{\mathfrak{z}} + \sigma J(\overline{\mathfrak{q}})^\top\dot{\mathfrak{e}} + \sigma\dot{J}(\overline{\mathfrak{q}})^\top\mathfrak{e}\right] \\
&= \left[\mathfrak{e} + \sigma J(\overline{\mathfrak{q}})\mathfrak{r}\right]^\top\dot{\mathfrak{e}} + \mathfrak{r}^\top\dot{\mathfrak{z}} + \sigma\mathfrak{r}^\top\dot{J}(\overline{\mathfrak{q}})^\top\mathfrak{e} = -\sigma\mathfrak{e}^\top J^+(\overline{\mathfrak{q}})\mathfrak{e} \\
&\quad + \mathfrak{e}^\top\mathfrak{b}(\cdot) + \sigma\mathfrak{r}^\top J(\overline{\mathfrak{q}})^\top\mathfrak{b}(\cdot) + \mathfrak{e}^\top J(\overline{\mathfrak{q}})\mathfrak{r} + \sigma\mathfrak{r}^\top J^+(\overline{\mathfrak{q}})\mathfrak{r} \\
&\quad + \sigma\mathfrak{r}^\top\dot{J}(\overline{\mathfrak{q}})^\top\mathfrak{e} + \mathfrak{r}^\top\mathfrak{l}(\cdot) + \mathfrak{r}^\top(\mathfrak{u} - \overline{u}) + \mathfrak{r}^\top d(\cdot).
\end{aligned} \tag{20}$$

By invoking (19) as well as the following:

$$\begin{aligned}
\sigma\mathfrak{r}^\top J(\overline{\mathfrak{q}})^\top\mathfrak{b}(\cdot) &\leq \sigma\|\mathfrak{r}\|_2\|J(\overline{\mathfrak{q}})\|_2\|\mathfrak{b}(\cdot)\|_2 \leq \sigma L_{\mathfrak{c}}\overline{J}\|\mathfrak{e}\|_2\|\mathfrak{r}\|_2, \\
\mathfrak{e}^\top J(\overline{\mathfrak{q}})\mathfrak{r} &\leq \|\mathfrak{e}\|_2\|J(\overline{\mathfrak{q}})\|_2\|\mathfrak{r}\|_2 \leq \overline{J}\|\mathfrak{e}\|_2\|\mathfrak{r}\|_2, \\
\sigma\mathfrak{r}^\top J^+(\overline{\mathfrak{q}})\mathfrak{r} &\leq \sigma\|\mathfrak{r}\|_2^2\|J^+(\overline{\mathfrak{q}})\|_2 \leq \sigma\|\mathfrak{r}\|_2^2\|J(\overline{\mathfrak{q}})\|_2\left\|J^\top(\overline{\mathfrak{q}})\right\|_2 \\
&\leq \sigma\overline{J}^2\|\mathfrak{r}\|_2^2, \\
\sigma\mathfrak{r}^\top\dot{J}(\overline{\mathfrak{q}})^\top\mathfrak{e} &\leq \sigma\|\mathfrak{e}\|_2\|\dot{J}(\overline{\mathfrak{q}})\|_2\|\mathfrak{r}\|_2 \leq \sigma\widetilde{J}\|\mathfrak{e}\|_2\|\mathfrak{r}\|_2 \\
\mathfrak{r}^\top\mathfrak{l}(\cdot) &\leq L\|\mathfrak{e}\|_2\|\mathfrak{r}\|_2 + L\|\mathfrak{r}\|_2^2, \\
\mathfrak{r}^\top d(\cdot) &\leq \|\mathfrak{r}\|_2\|d(\cdot)\|_2 \leq \|\mathfrak{y}\|_2\widetilde{d},
\end{aligned}$$

(20) becomes:

$$\dot{\mathfrak{L}}(\mathfrak{y}) \leq -\underline{\sigma}\|\mathfrak{e}\|_2^2 + \Lambda_1\|\mathfrak{e}\|_2\|\mathfrak{r}\|_2 + \Lambda_2\|\mathfrak{r}\|_2^2 + \mathfrak{r}^\top(\mathfrak{u}-\overline{u}) + \|\mathfrak{y}\|_2\widetilde{d}. \quad (21)$$

with Λ_1, Λ_2 given in (15b). By using Lemma 1 for $n = P = 1$, we get $\|\mathfrak{e}\|_2\|\mathfrak{r}\|_2 \leq \frac{1}{4\rho}\|\mathfrak{e}\|_2^2 + \rho\|\mathfrak{r}\|_2^2$, with ρ designed so that (15a) holds. Combining the latter with (21) it yields:

$$\dot{\mathfrak{L}}(\mathfrak{y}) \leq -\left(\underline{\sigma} - \tfrac{\Lambda_1}{4\rho}\right)\|\mathfrak{e}\|_2^2 + \left(\rho\Lambda_1 + \Lambda_2\right)\|\mathfrak{r}\|_2^2 + \mathfrak{r}^\top(\mathfrak{u}-\overline{u}) + \|\mathfrak{y}\|_2\widetilde{d}.$$

By designing $\mathfrak{u} - \overline{u} = -k\mathfrak{r} = -k\mathfrak{e} - k\sigma J(\overline{\mathfrak{q}})^\top\mathfrak{z}$, which is compatible with (12) and the same as in (14), we have:

$$\begin{aligned}\dot{\mathfrak{L}}(\mathfrak{y}) &\leq -\left(\underline{\sigma} - \tfrac{\Lambda_1}{4\rho}\right)\|\mathfrak{e}\|_2^2 - \left(k - \rho\Lambda_1 - \Lambda_2\right)\|\mathfrak{r}\|_2^2 + \|\mathfrak{y}\|_2\widetilde{d} \\ &\leq -\min\{\alpha_1,\alpha_2\}\|\mathfrak{y}\|_2^2 + \|\mathfrak{y}\|_2\widetilde{d} \\ &= -\|\mathfrak{y}\|_2\big[\min\{\alpha_1,\alpha_2\}\|\mathfrak{y}\|_2 - \widetilde{d}\big],\end{aligned}$$

as α_1 and α_2 given in (17). Thus, $\dot{\mathfrak{L}}(\mathfrak{y}) < 0$, when $\|\mathfrak{y}\|_2 > \frac{\widetilde{d}}{\min\{\alpha_1,\alpha_2\}}$. Taking the latter into consideration and the fact that $\mathfrak{y}(0)$, we have that $\|\mathfrak{y}(t)\| \leq \frac{\widetilde{d}}{\min\{\alpha_1,\alpha_2\}}$, $\forall t \geq 0$. Moreover, the following inequalities hold:

$$\begin{aligned}&\|\mathfrak{e}\|_2 \leq \|\mathfrak{y}\|_2 \Rightarrow \|\mathfrak{e}(t)\|_2 \leq \tfrac{\widetilde{d}}{\min\{\alpha_1,\alpha_2\}}, \forall t \geq 0, \\ &\Big|\|\mathfrak{e}\|_2 - \big\|J^\top\mathfrak{z}\big\|_2\Big| \leq \big\|\mathfrak{e} + J^\top\mathfrak{z}\big\|_2 = \|\mathfrak{z}\|_2 \leq \|\mathfrak{y}\|_2 \\ &\Rightarrow \|\mathfrak{z}(t)\|_2 \leq \tfrac{2\widetilde{d}}{\overline{J}\min\{\alpha_1,\alpha_2\}}, \forall t \geq 0.\end{aligned}$$

Remark 1. According to Lemma 2, the volume of the tube which is centered along the nominal trajectories $\overline{e}(t), \overline{\zeta}(t)$, that are solution of system (11a),(11b), depends on the parameters $\widetilde{d}$, $\overline{J}$, $\underline{J}$, $\widetilde{J}$, L and L_ϵ. By tuning the parameters ρ and k from (15a) appropriately, the volume of the tube can be adjusted.

C. On-line Optimal Control

Consider a sequence of sampling times $\{t_k\}$, $k \in \mathbb{N}$, with a constant sampling period $0 < h < T$, where T is a prediction horizon such that $t_{k+1} := t_k + h$, $\forall k \in \mathbb{N}$. At each sampling time t_k, a FHOCP is solved as follows:

$$\min_{\overline{u}(\cdot)}\left\{\|\overline{\xi}(t_k+T)\|_P^2 + \int_{t_k}^{t_k+T}\Big[\|\overline{\xi}(\mathfrak{s})\|_Q^2 + \|\overline{u}(\mathfrak{s})\|_R^2\Big]d\mathfrak{s}\right\} \quad (22a)$$

subject to:

$$\dot{\overline{\xi}}(\mathfrak{s}) = g(\overline{\xi}(\mathfrak{s}),\overline{u}(\mathfrak{s})), \quad \overline{\xi}(t_k) = \xi(t_k), \quad (22b)$$

$$\overline{\xi}(\mathfrak{s}) \in \overline{\mathcal{E}} \times \overline{\mathcal{Z}}, \quad \overline{u}(\mathfrak{s}) \in \overline{\mathcal{U}}, \quad \forall \mathfrak{s} \in [t_k, t_k+T], \quad (22c)$$

$$\overline{\xi}(t_k+T) \in \mathcal{F}, \quad (22d)$$

where $\xi := [e^\top, \zeta^\top]^\top \in \mathbb{R}^{12+n}$, $g(\xi,u) := \begin{bmatrix} J(\mathfrak{q})\zeta \\ f(e+\chi_{\text{des}},\zeta)+u\end{bmatrix}$; Q, $P \in \mathbb{R}^{(12+n)\times(12+n)}$ and $R \in \mathbb{R}^{(6+n)\times(6+n)}$ are positive definite gain matrices to be appropriately tuned. We will explain hereafter the sets $\overline{\mathcal{E}}$, $\overline{\mathcal{V}}$, $\overline{\mathcal{U}}$ and $\mathcal{F}$.

In order to guarantee that while the FHOCP (22a)-(22d) is solved for the nominal dynamics (11a)-(11b), the real states e, ζ and control input $\mathfrak{u}$ satisfy the corresponding state $\mathcal{E}$, $\mathcal{Z}$ and input constraints $\mathcal{U}$, respectively, the following modification is performed: $\overline{\mathcal{E}} := \mathcal{E} \ominus \Omega_1$, $\overline{\mathcal{Z}} := \mathcal{Z} \ominus \Omega_2$, $\overline{\mathcal{U}} := \mathcal{U} \ominus \big[\Lambda \circ \overline{\Omega}\big]$, with $\Lambda := \text{diag}\{-kI_6, -k\sigma\overline{J}I_{6+n}\} \in \mathbb{R}^{(12+n)\times(12+n)}$, $\overline{\Omega} := \Omega_1 \times \Omega_2$, the operators $\ominus$, $\circ$ as defined in Section II, and Ω_1, Ω_2 as given in (16a), (16b), respectively. Intuitively, the sets $\mathcal{E}$, $\mathcal{Z}$ and $\mathcal{U}$ are tightened accordingly, in order to guarantee that while the nominal states $\overline{e}$, $\overline{\zeta}$ and the nominal control input $\overline{u}$ are calculated, the corresponding real states e, ζ and real control input $\mathfrak{u}$ satisfy the state and input constraints $\mathcal{E}$, $\mathcal{Z}$ and $\mathcal{U}$, respectively. This constitutes a standard constraints set modification technique adopted in tube-based NMPC frameworks (for more details see [19]). Define the *terminal set* by:

$$\mathcal{F} := \big\{\overline{\xi} \in \overline{\mathcal{E}} \times \overline{\mathcal{Z}} : \|\overline{\xi}\|_P \leq \epsilon\big\}, \quad \epsilon > 0, \quad (23)$$

which is used to enforce the stability of the system [14]. In particular, due to the fact that the linearized nominal dynamics $\dot{\overline{\xi}} = A\overline{\xi} + B\overline{u}$ are stabilizable, it can be proven that (see [14, Lemma 1, p. 4]) there exists a *local controller* $u_{\text{loc}} := \mathfrak{K}\overline{\xi} \in \overline{\mathcal{U}}$, $\mathfrak{K} \in \mathbb{R}^{(6+n)\times(6+n)}$, $\mathfrak{K} > 0$ which guarantees that: $\frac{d}{dt}\left(\|\overline{\xi}\|_P^2\right) \leq -\|\overline{\xi}\|_{\widetilde{Q}}^2$, $\forall \overline{\xi} \in \mathcal{F}$, with $\widetilde{Q} := Q + \mathfrak{K}^\top R\mathfrak{K}$.

Theorem 1. *Suppose also that the FHOCP* (22a)-(22d) *is feasible at time* $t = 0$. *Then, the feedback control law* (12) *applied to the system* (10a)-(10b) *guarantees that there exists a time* $\mathfrak{t}$ *such that* $\forall t \geq \mathfrak{t}$ *it holds that:*

$$\|\chi(t) - \chi_{\text{des}}\|_2 \leq \tfrac{\epsilon}{\sqrt{\lambda_{\min}(P)}} + \tfrac{\widetilde{d}}{\min\{\alpha_1,\alpha_2\}}, \quad (24a)$$

$$\|\zeta(t)\|_2 \leq \tfrac{\epsilon}{\sqrt{\lambda_{\min}(P)}} + \tfrac{2\widetilde{d}}{\overline{J}\min\{\alpha_1,\alpha_2\}}. \quad (24b)$$

Proof. The proof of the theorem consists of two parts:
Feasibility Analysis: It can be shown that recursive feasibility is established and it implies subsequent feasibility. The proof of this part is similar to the feasibility proof of [8, Theorem 2, Sec. 4, p. 12], and it is omitted here due to space constraints.
Convergence Analysis: Recall that $e = \chi - \chi_{\text{des}}$, $\mathfrak{e} = e - \overline{e}$ and $\mathfrak{z} = \zeta - \overline{\zeta}$. Then, we get $\|\chi(t) - \chi_{\text{des}}\|_2 \leq \|\overline{e}(t)\|_2 + \|\mathfrak{e}(t)\|_2$, $\|\zeta(t)\|_2 \leq \|\overline{\zeta}(t)\|_2 + \|\mathfrak{z}(t)\|_2$, which, by using the fact that $\|\overline{e}\|$, $\|\overline{\zeta}\| \leq \|\overline{\xi}\|_2$ as well as the bounds from (16a), (16b) the latter inequalities become:

$$\|\chi(t) - \chi_{\text{des}}\|_2 \leq \|\overline{\xi}(t)\|_2 + \tfrac{\widetilde{d}}{\min\{\alpha_1,\alpha_2\}}, \quad (25a)$$

$$\|\zeta(t)\|_2 \leq \|\overline{\xi}(t)\|_2 + \tfrac{2\widetilde{d}}{\overline{J}\min\{\alpha_1,\alpha_2\}}, \forall t \geq 0. \quad (25b)$$

The nominal state $\overline{\xi}$ is controlled by the nominal control action $\overline{u} \in \overline{\mathcal{U}}$ which is the outcome of the solution to the FHOCP (22a)-(22d) for the nominal dynamics (11a)-(11b). Hence, by invoking previous NMPC stability results found in [14], the state $\overline{\xi}(t)$ is driven to terminal set $\mathcal{F}$, given in (23), in finite time, and it remains there for all times. Thus, there exist a finite time $\mathfrak{t}$ such that $\overline{\xi}(t) \in \mathcal{F}$, $\forall t \geq \mathfrak{t}$. From (23), the latter implies that: $\|\overline{\xi}(t)\|_P \leq \epsilon, \forall t \geq \mathfrak{t} \Rightarrow \|\overline{\xi}(t)\|_2 \leq \frac{\epsilon}{\sqrt{\lambda_{\min}(P)}}, \forall t \geq \mathfrak{t}$. The latter implication combined by (25a)-(25b) leads to the conclusion of the proof. □

□

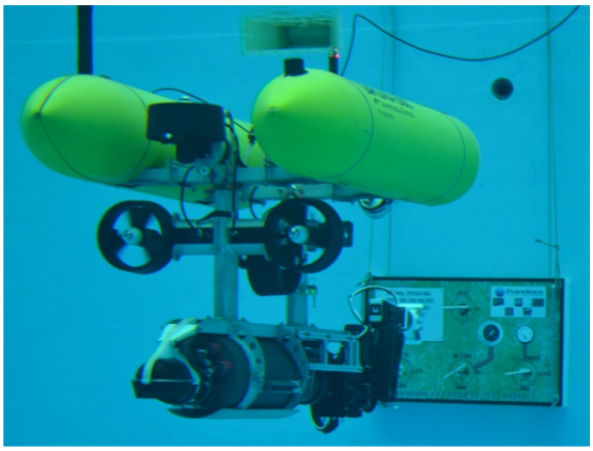

Fig. 2: The GIRONA-UVMS composed of Girona500 AUV and ARM 5E Micro manipulator [4].

	$d_i(m)$	q_i	$a_i(m)$	α_i(rad)
1	0	q_1	0.1	$-\frac{\pi}{2}$
2	0	q_2	0.26	0
3	0	q_3	0.09	$\frac{\pi}{2}$
4	0.29	q_4	0	0
E	$\text{Rot}(y, -\frac{\pi}{2})$			

TABLE I: Denavit-Hantenberg Parameters of the ARM 5E Micro

V. Simulation Results

For a simulation scenario, consider the Girona 500 AUV depicted in Fig. 2 equipped with an ARM 5E Micro manipulator from [4]. The manipulator consists of $n = 4$ revolute joints with limits: $-0.52 \leq q_1 \leq 1.46$, $0.1471 \leq q_2 \leq 1.3114$, $-1.297 \leq q_3 \leq 0.73$ and $-3.14 \leq q_4 \leq 3.14$. The end-effector is in ready-to-grasp mode with initial state: $\chi(0) = [\mathfrak{p}(0)^\top, \mathfrak{o}(0)^\top]^\top = [-1.0, 1.3, -1.0, 0.0, -\frac{\pi}{8}, \frac{\pi}{12}]^\top$. The stiffness matrix is $K = I_6$ with $\chi_{\text{eq}} = 0$ which results to $\mathfrak{F}_{\text{des}} = \chi_{\text{des}} = [\mathfrak{p}_{\text{des}}^\top, \mathfrak{o}_{\text{des}}^\top]^\top = [0, 0, 0, \frac{\pi}{3}, \frac{\pi}{10}, 0]^\top$. According to (2), the transformation matrices which lead to the forward kinematics are given by:

$$T_B^I = \begin{bmatrix} \mathfrak{J}_1(\eta_2) & \eta_1 \\ 0_{1\times 3} & 1 \end{bmatrix}, \quad T_0^B = \begin{bmatrix} I_{3\times 3} & [0.53, 0, 0.36]^\top \\ 0_{1\times 3} & 1 \end{bmatrix},$$

and T_i^{i-1}, $i = 1, \ldots, 4$ are given by the Denavit-Hantenberg parameters which can be calculated from Table I. By imposing the constraints $-\pi \leq \phi, \psi \leq \pi$ and $-\frac{\pi}{2} + \epsilon \leq \theta \leq \frac{\pi}{2} - \epsilon$, $\epsilon = 0.1$, according to (7) we get $\underline{J} = 0.5095$ and $L_\epsilon = 2\sqrt{2}$. For simplified calculations, we apply the methodology of this paper by considering disturbance in the following disturbed kinematic model: $\dot{\chi} = J(\mathfrak{q})\zeta + w(\mathfrak{q}, t)$, with $w(\cdot) = 0.2\sin(t)I_6 \Rightarrow \|w(\cdot)\|_2 \leq 0.2 = \widetilde{w}$, in which the vector ζ stands for the virtual control input to be designed such that $\lim_{t\to\infty} \|\chi(t) - \chi_{\text{des}}\| \to 0$. The input constraints are set to $\|\nu_1\|_2 \leq 2$, $\|\nu_2\|_2 \leq 2$ and $\|\dot{q}\|_2 \leq 2$. Then, by using (13a) and (18) and designing the control gain $\sigma = 3.084$, the resulting RCI is $\Omega = \left\{\mathfrak{e} \in \mathbb{R}^6 : \|\mathfrak{e}\|_2 \leq \frac{\widetilde{w}}{\sigma\underline{J} + L_\epsilon} = 0.3\right\}$. The simulation time is 6 sec. The optimization horizon and the sampling time

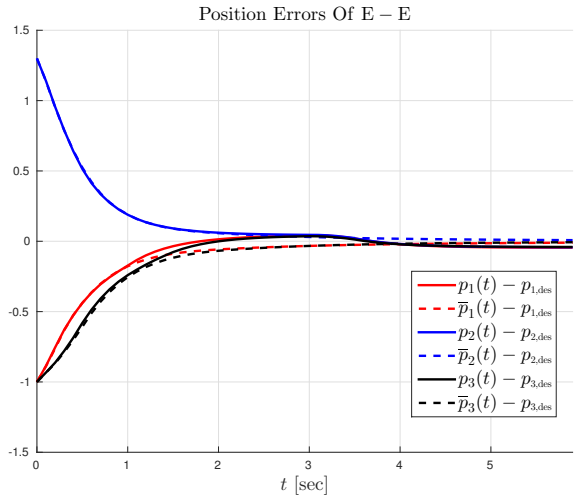

Fig. 3: The evolution of the real position errors of the end-effector $\mathfrak{p}_1(t) - \mathfrak{p}_{1,\text{des}}$, $\mathfrak{p}_2(t) - \mathfrak{p}_{2,\text{des}}$, $\mathfrak{p}_3(t) - \mathfrak{p}_{3,\text{des}}$ depicted with solid lines as well as the corresponding nominal position errors $\bar{\mathfrak{p}}_1(t) - \mathfrak{p}_{1,\text{des}}$, $\bar{\mathfrak{p}}_2(t) - \mathfrak{p}_{2,\text{des}}$, $\bar{\mathfrak{p}}_3(t) - \mathfrak{p}_{3,\text{des}}$ depicted with dashed lines.

are set to $T = 0.7\,\text{sec}$ and $h = 0.1\,\text{sec}$, respectively. The NMPC gains are set to $Q = P = 0.5I_6$ and $R = 0.5I_{10}$. Fig. 3 shows the evolution of the real and the nominal position errors of the end-effector. the corresponding real and nominal orientation errors are depicted in Fig. 4. Finally, the control inputs are presented in Fig. 5. It can be observed that the desired task is performed while all the state/input constraints are satisfied.

VI. Conclusions and Future Research

This paper addresses the problem of force/torque control of UVMS under state/input constraints as well as external uncertainties/disturbances. In particular, we have proposed a tube-based robust NMPC framework that incorporates the aforementioned constraints in a novel way. Future efforts will be devoted towards extending the current framework under multi-UVMS which interact with each other through a common object in order to perform a collaborative manipulation task. Another topic of static will be the control of the UVMS under high-level tasks [22]–[26]. Lastly, application of existing formation control frameworks [27]–[29] to UVMS will be considered.

References

[1] G. Antonelli, "Underwater Robots," *Springer Tracts in Advanced Robotics*, 2013.

[2] S. Heshmati-alamdari, A. Nikou, K. J. Kyriakopoulos, and D. V. Dimarogonas, "A Robust Force Control Approach for Underwater Vehicle Manipulator Systems," *20th World Congress of the International Federation of Automatic Control (IFAC WC), Toulouse, France*, pp. 11197–11202, 2017.

[3] S. Heshmati-alamdari, C. Bechlioulis, G. Karras, A. Nikou, D. V. Dimarogonas, and K. J. Kyriakopoulos, "A Robust Interaction Control Approach for Underwater Vehicle Manipulator Systems," *Annual Reviews in Control*, 2018.

[4] P. Cieslak, P. Ridao, and M. Giergiel, "Autonomous Underwater Panel Operation by GIRONA500 UVMS: A Practical Approach to Autonomous Underwater Manipulation," *IEEE International Conference on Robotics and Automation (ICRA)*, pp. 529–536, 2015.

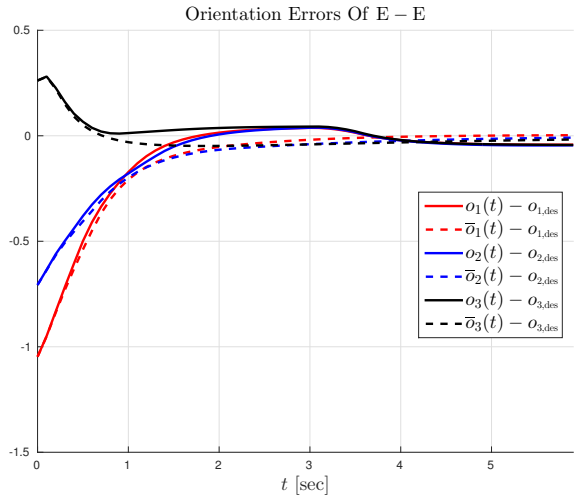

Fig. 4: The evolution of the real orientation errors $\mathfrak{o}_1(t) - \mathfrak{o}_{1,\text{des}}$, $\mathfrak{o}_2(t) - \mathfrak{o}_{2,\text{des}}$, $\mathfrak{o}_3(t) - \mathfrak{o}_{3,\text{des}}$ depicted with solid lines as well as the corresponding nominal orientation errors $\bar{\mathfrak{o}}_1(t) - \mathfrak{o}_{1,\text{des}}$, $\bar{\mathfrak{o}}_2(t) - \mathfrak{o}_{2,\text{des}}$, $\bar{\mathfrak{o}}_3(t) - \mathfrak{o}_{3,\text{des}}$ depicted with dashed lines.

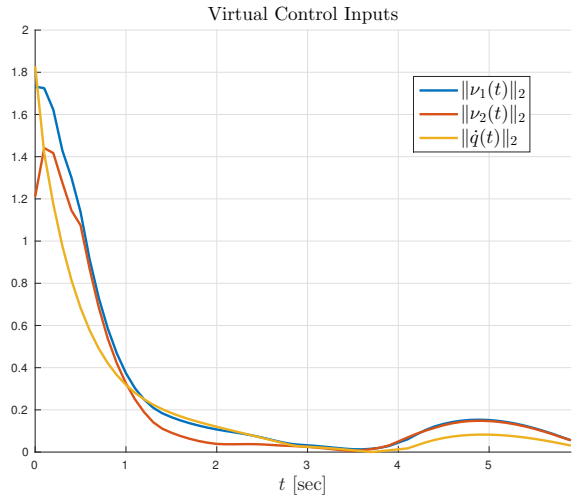

Fig. 5: The virtual control input signals $\|\nu_1(t)\|_2$, $\|\nu_2(t)\|_2$ and $\|\dot{q}(t)\|_2$ of the kinematic model (3). It holds that $\|\nu_1\|_2 \leq 2$, $\|\nu_2\|_2 \leq 2$ and $\|\dot{q}\|_2 \leq 2$.

[5] A. Nikou, C. K. Verginis, S. Heshmati, and D. V. Dimarogonas, "A Nonlinear Model Predictive Control Scheme for Cooperative Manipulation with Singularity and Collision Avoidance," *25th IEEE Mediterranean Conference on Control and Automation (MED)*, pp. 707–712, Valletta, Malta, 2017.

[6] S. Heshmati-alamdari, G. Karras, P. Marantos, and K. J. Kyriakopoulos, "A Robust Model Predictive Control Approach for Autonomous Underwater Vehicles Operating in a Constrained Workspace," *2018 IEEE International Conference on Robotics and Automation (ICRA)*, pp. 1–5, 2018.

[7] C. K. Verginis, A. Nikou, and D. V. Dimarogonas, "Communication-based Decentralized Cooperative Object Transportation Using Nonlinear Model Predictive Control," *European Control Conference (ECC), ArXiv Link: https://arxiv.org/abs/1803.07940*, 2018.

[8] A. Nikou and D. V. Dimarogonas, "Decentralized Tube-based Model Predictive Control of Uncertain Nonlinear Multi-Agent Systems," *International Journal of Robust and Nonlinear Control (IJRNC), ArXiv: https://arxiv.org/abs/1808.05408*, 2018, (under review).

[9] *The Society of Naval Architects and Marine Engineers, Nomenclature for treating the motion of a submerged body through a fluid (Technical and Research Bulletin)*, 1950.

[10] L. Sciavicco and B. Siciliano, "Modelling and Control of Robot Manipulators," *Springer Science & Business Media*, 2012.

[11] A. Nikou, G. Gavridis, and K. J. Kyriakopoulos, "Mechanical Design, Modelling and Control of a Novel Aerial Manipulator," *2018 IEEE International Conference on Robotics and Automation (ICRA)*, pp. 4698–4703, Seattle, USA, 2015.

[12] B. Siciliano and L. Villani, "Robot force Control," *International Series in Engineering and Computer Science. Robotics: Vision, Manipulation and Sensors*, 1999.

[13] H. Michalska and D. Mayne, "Robust Receding Horizon Control of Constrained Nonlinear Systems," *IEEE Transactions on Automatic Control (TAC)*, vol. 38, no. 11, pp. 1623–1633, 1993.

[14] H. Chen and F. Allgöwer, "A Quasi-Infinite Horizon Nonlinear Model Predictive Control Scheme with Guaranteed Stability," *Automatica*, vol. 34, no. 10, pp. 1205–1217, 1998.

[15] D. Mayne, J. Rawlings, C. Rao, and P. Scokaert, "Constrained Model Predictive Control: Stability and Optimality," *Automatica*, vol. 36, no. 6, pp. 789–814, 2000.

[16] A. Filotheou, A. Nikou, and D. V. Dimarogonas, "Robust Decentralized Navigation of Multi-Agent Systems with Collision Avoidance and Connectivity Maintenance Using Model Predictive Controllers," *International Journal of Control (IJC), Available Online: https://www.tandfonline.com/doi/full/10.1080/00207179.2018.1514129*, 2018.

[17] A. Filotheou, A. Nikou, and D. V. Dimarogonas, "Decentralized Control of Uncertain Multi-Agent Systems with Connectivity Maintenance and Collision Avoidance," *European Control Conference (ECC), ArXiv Link: https://arxiv.org/abs/1710.09204*, 2018.

[18] A. Nikou, S. Heshmati-alamdari, C. K. Verginis, and D. V. Dimarogonas, "Decentralized Abstractions and Timed Constrained Planning of a General Class of Coupled Multi-Agent Systems," *56th IEEE Conference on Decision and Control (CDC)*, pp. 990–995, Melbourne, Australia, 2017.

[19] S. Yu, C. Maier, H. Chen, and F. Allgöwer, "Tube MPC Scheme Based on Robust Control Invariant Set with Application to Lipschitz Nonlinear Systems," *Systems and Control Letters*, vol. 62, no. 2, pp. 194–200, 2013.

[20] A. Nikou and D. V. Dimarogonas, "Robust Tube-based Model Predictive Control for Timed-constrained Robot Navigation," *American Control Conference (ACC), ArXiv: https://arxiv.org/abs/1809.09825*, 2018, (under review).

[21] M. Krstic, I. Kanellakopoulos, and P. Kokotovic, "Nonlinear and Adaptive Control Design," *Publisher: Wiley New York*, 1995.

[22] A. Nikou, J. Tumova, and D. Dimarogonas, "Cooperative Task Planning of Multi-Agent Systems Under Timed Temporal Specifications," *American Control Conference (ACC), Boston, USA*, pp. 13–19, 2016.

[23] A. Nikou, D. Boskos, J. Tumova, and D. V. Dimarogonas, "Cooperative Planning Synthesis for Coupled Multi-Agent Systems Under Timed Temporal Specifications," *American Control Conference (ACC), Seattle, USA*, pp. 1847–1852, 2017.

[24] S. Andersson, A. Nikou, and D. V. Dimarogonas, "Control Synthesis for Multi-Agent Systems under Metric Interval Temporal Logic Specifications," *20th World Congress of the International Federation of Automatic Control (IFAC WC), Toulouse, France*, vol. 50, Issue 1, pp. 2397–2402, 2017.

[25] A. Nikou, D. Boskos, J. Tumova, and D. V. Dimarogonas, "On the Timed Temporal Logic Planning of Coupled Multi-Agent Systems," *Automatica*, vol. 97, pp. 339–345, 2018.

[26] A. Nikou, J. Tumova, and D. V. Dimarogonas, "Probabilistic Plan Synthesis for Coupled Multi-Agent Systems," *20th World Congress of the International Federation of Automatic Control (IFAC WC), Toulouse, France*, vol. 50, Issue 1, pp. 10766–10771, 2017.

[27] C. K. Verginis, A. Nikou, and D. V. Dimarogonas, "Position and Orientation Based Formation Control of Multiple Rigid Bodies with Collision Avoidance and Connectivity Maintenance," *56th IEEE Conference on Decision and Control (CDC)*, pp. 411–416, Melbourne, Australia, 2017.

[28] A. Nikou, C. K. Verginis, and D. V. Dimarogonas, "Robust Distance-Based Formation Control of Multiple Rigid Bodies with Orientation Alignment," *20th World Congress of the International Federation of Automatic Control (IFAC WC), Toulouse, France*, pp. 15458–15463, 2017.

[29] C. K. Verginis, A. Nikou, and D. V. Dimarogonas, "Robust Formation Control in SE(3) for Tree-Graph Structures with Prescribed Transient and Steady State Performance," *Automatica, ArXiv Link: https://arxiv.org/abs/1803.07513*, (Under Review), 2018.